Depolarization of Interacting NV ensembles : The Role of Local Electric Fields and Double Flip processes

C. Pellet-Mary[1], M. Perdriat[1], P. Huillery[?], G. Hétet[1]

[1] *Laboratoire De Physique de l'École Normale Supérieure, École Normale Supérieure, PSL Research University, CNRS, Sorbonne Université, Université Paris Cité , 24 rue Lhomond, 75231 Paris Cedex 05, France.*

We present experimental results on dipolar interaction processes in ensemble of spin-1 systems. Using the spin of highly doped ensembles of negatively charged nitrogen vacancy centers in diamonds, we identify regimes where flip-flop, double-flip processes as well as the mixing induced by local electric field dominate. Our results are relevant for understanding decoherence in many-body spin systems as well as for high sensitivity magneto- and electro-metry with long-lived interacting solid-state spins. As a proof of principle, we present an orientation-free and microwave-free magnetometer operating with a sensitivity below 100 nT/$\sqrt{\text{Hz}}$.

The electronic spin properties of the negatively charged nitrogen-vacancy (NV^-) center in diamond has given rise to a wealth of applications in nanoscale sensing and quantum information science in part thanks to the possibility to optically polarize and read-out its spin state at ambient conditions. Many recent work indeed focus on ensembles of spins from NV centers with the prospect to boost the magnetic field sensing capabilities and for studying many body effects [3, 6, 11, 14, 24]

When the spin ensemble becomes dense, inhomogeneities in the relaxation rates of NVs can give rise to spin depolarisation with a very rich many body dynamics associated with disorder. This mechanisms however limits the efficiency of magnetometers [28] Recent magnetometry proposals have been put forward at zero magnetic field. There, the depolarisation effect was shown to be much stronger, but the detailed studies of relaxation mechanisms have not been identified to the best of our knowledge. Some of the possible processes that lead to cross-relaxation in strongly coupled dipolar systems are depicted in Fig. 1. The goal of this paper is to identify regimes where the spin flip-flop within different classes of NV centers, double-flip up and down as well as the mixing induced by local electric field play a role.

The electronic spin of NV center is a spin-1 system in the ground state (see Fig. 1). It can be optically polarized in the $|m_s = 0\rangle$ state. The photoluminescence of this state is also is larger than the $|m_s = \pm 1\rangle$ states enabling spin-read out at ambient temperature. The $|m_s = \pm 1\rangle$ spin states are separated from the $|m_s = 0\rangle$ state by $D = (2\pi)2.87$ GHz so that when a resonant microwave or static transverse magnetic field is applied, the photoluminescence is reduced [7, 15]. Fig. 2-a) and b) show the change in photoluminescence (PL) with respect to an external magnetic field for two samples with a low and high concentration of NV^- centers (see SI). Both samples show a decrease in PL as the magnetic field amplitude increases. There is however a stark difference in the low magnetic field region where only high-density samples shows a drop in PL [13, 18]. This effect can be observed on all our samples (see SI) whenever the NV

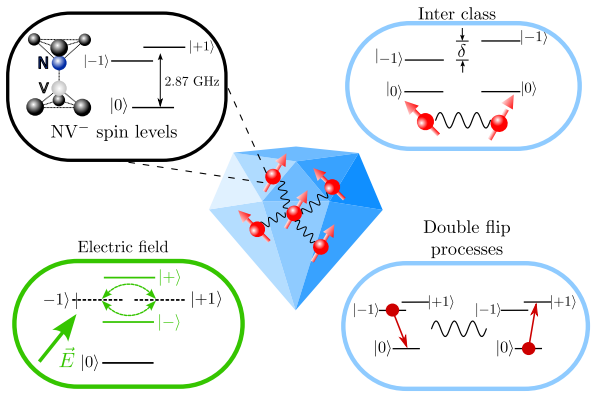

FIG. 1. Schematics showing a diamond with interacting spins as well as the three processes that can account for dipolar relaxation.

concentration lies in the ppm range. The drop of the PL at low magnetic field is associated with a decrease of the NV's spin lifetime T_1 [12], which results in a decrease of the population in the bright state $|0\rangle$.

The depolarization dynamics of the spin of single or dilute NV centers at room temperature is dominated by two-phonon Raman processes [12, 19, 23], which depend on the crystal lattice temperature. It has been observed that dense NV centers ensemble have an additional spin decay channel [1, 2, 4, 12, 13, 17, 18, 20], which depends greatly on the magnetic field amplitude. This effect has been attributed to cross-relaxation between the NV centers through dipole-dipole coupling [4, 18]. Inhomogeneity of the spin lifetimes is further needed in order to explain the depolarization of the spin ensemble. We will denote T_1^{ph} the characteristic timescale associated with the phonon relaxation process and T_1^{dd} the density dependent timescale associated with the dipole-dipole relaxation process.

Fig. 2-c) shows the sequence employed for measuring T_1^{dd} in the dense sample. It consists in a pump-probe measurement where the spins are first polarized in the $|0\rangle$ state by a green laser, and read-out optically after

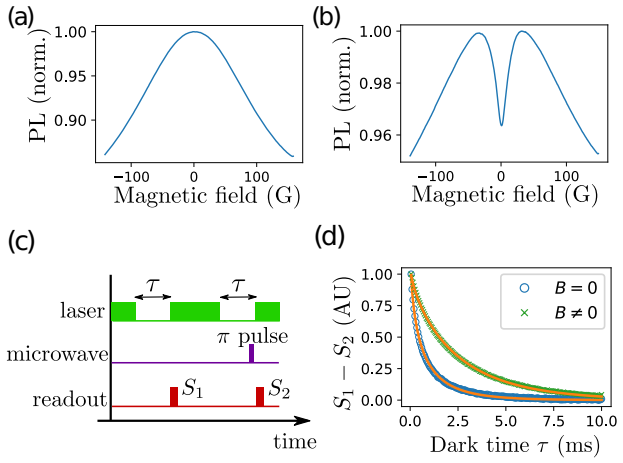

FIG. 2. a) Photoluminescence measurement from NV centers ensemble as a function of an external magnetic field applied in an arbitrary direction (a) for the sample CVD-PPB, with $[NV^-] \approx 50$ ppb (b) for the sample HPHT-150-1, with $[NV^-] \approx 3$ ppm. (c) Sequence used to measure the spin lifetime. (d) Spin relaxation $S_1 - S_2$ measured for the dense sample at zero and non-zero magnetic fields. The fitting procedure (orange plain line) is detailed in the main text

a variable dark time τ. In highly doped samples, this sequence often results in artifacts, mostly due to charge state transfer in the dark [10, 11]. It is therefore convenient to repeat the sequence with an additional π pulse right before the spin read-out to prepare the remaining $|0\rangle$ polarization into a darker $|+1\rangle$ or $|-1\rangle$ state. By subtracting the result of the two sequences, we select only the spin-dependent part of the signal, with the added benefit of being able to select a specific class of NV centers [4, 12, 18].

Fig. 2-b) shows the subtracted signals when $\boldsymbol{B} = 0$ and $\boldsymbol{B} \neq 0$. The ensemble spin decay curves are not exponential, which was found to be due to inhomogeneities between the spin lifetimes of dipolar coupled NV^- centers [4]. We will base our interpretations of the experimental results on the NV-fluctuator model developed in [4]. A conclusion of this model is that, for a homogeneous 3D distribution of fluctuators, the dipole-induced lifetime should be stretched-exponential with a stretch factor $\beta = 1/2$. Such an ensemble lifetime is indeed observed when $T_1^{\mathrm{dd}} \ll T_1^{\mathrm{ph}}$. For the samples used in this paper (detailed in SI) $T_1^{\mathrm{dd}} \sim T_1^{\mathrm{ph}}$, so both decay processes have to be included in the analysis. Fitting the two curves by the product of an exponential and a stretched exponential, we find $T_1^{\mathrm{ph}} = 3.6$ ms for both and $T_1^{\mathrm{dd}} = 0.6$ ms and 13.0 ms respectively. We also conducted further measurements that confirm the lifetime-limited character of the fluctuator employed in the model [4], see SI.

One of the ways to tune dipole-dipole related phenomena is by changing the number of resonant spins. Fig. 3 (b)-i) shows an optically detected magnetic resonance (ODMR) spectrum from the dense ensemble HPHT-150-1. The observed lines correspond to the projections of the magnetic fields onto the four "classes" of NV centers - that is physical orientation of the NV axis is the diamond crystal cell - together with the two possible spin transitions $|0\rangle \rightarrow |-1\rangle$ and $|0\rangle \rightarrow |+1\rangle$. The transitions frequencies of the four different classes can be controlled by changing the amplitude and orientation of the external magnetic field. Fig. 3 (c)-i) shows an example where all four classes are brought to resonance by placing the magnetic field along the [100] crystalline axis. This configuration will be essential to decipher what dipolar relaxation mechanisms play a role at low field.

Fig. 3 (b)-ii) and (b)-iii) show the PL from an ensemble of NV centers as a function of the amplitude of a magnetic field aligned as in Fig. 3 (b)-i). We also extract the stretched exponential spin decay time T_1^{dd} by running the sequence shown in Fig. 2-c) at each of the 0.5 G magnetic field values. We observe that the 3 % increase in PL under low magnetic field is indeed correlated with a drop in the spin decay rate from 1.6 kHz to 0.08 kHz, as the magnetic field increases. This result can be explained by the higher number of resonant spins in zero magnetic field, where all four classes are degenerate, as opposed when $\boldsymbol{B} \neq 0$. The half width of the dip ($\approx$ 10G) is consistent with a fluctuator model taking into account the change in the spin resonance overlaps as the B field is swept (see SI ?) [Je sais pas, je le fais ?]. Note that the decrease in PL for $B > 40$ G are related to state mixing by the transverse magnetic field, so it is not correlated to a modification of the spin lifetime.

Importantly, we observed that the lifted degeneracy of the four NV classes is not the sole reason for the increase of the spin lifetime as the B field increases. Fig. 3 (c)-ii) and (c)-iii) show the change in the PL and in $1/T_1^{\mathrm{dd}}$ as a function of a magnetic field that is aligned along the [100] axis. For this particular orientation, the four classes are always resonant, regardless of the field amplitude. We can see that there still is an increase in the spin decay rate and a corresponding drop in the PL under low magnetic field values, although considerably reduced. The main aim of this paper is to understand the physics governing the contribution to the spin decay in this second scenario. Note that the slight drop in PL and the corresponding bump for $1/T_1^{\mathrm{dd}}$ at $B \sim 20$G is related to dipolar interaction with NV centers that have a ^{13}C as a first neighbor [21].

We identified and isolated two additional mechanisms that could explain this effect : local electric fields and double-flip processes. The dipole-dipole interaction Hamiltonian between two spins $\vec{S}_1$ and $\vec{S}_2$ reads :

$$\mathcal{H}^{\mathrm{dd}} = -\frac{J_0}{r^3}\left(3\left(\vec{S}_1 \cdot \vec{u}\right)\left(\vec{S}_2 \cdot \vec{u}\right) - \vec{S}_1 \cdot \vec{S}_2\right), \qquad (1)$$

Where $J_0 = (2\pi)52$ MHz $\cdot$ nm^3, $\vec{r}$ is the relative positions of the two spins and $\vec{u} = \frac{\vec{r}}{\|\vec{r}\|}$. In situations such as the one described in Fig.XX, the only relevant terms of $\mathcal{H}^{\mathrm{dd}}$ in terms of population transfer are the flip-flop

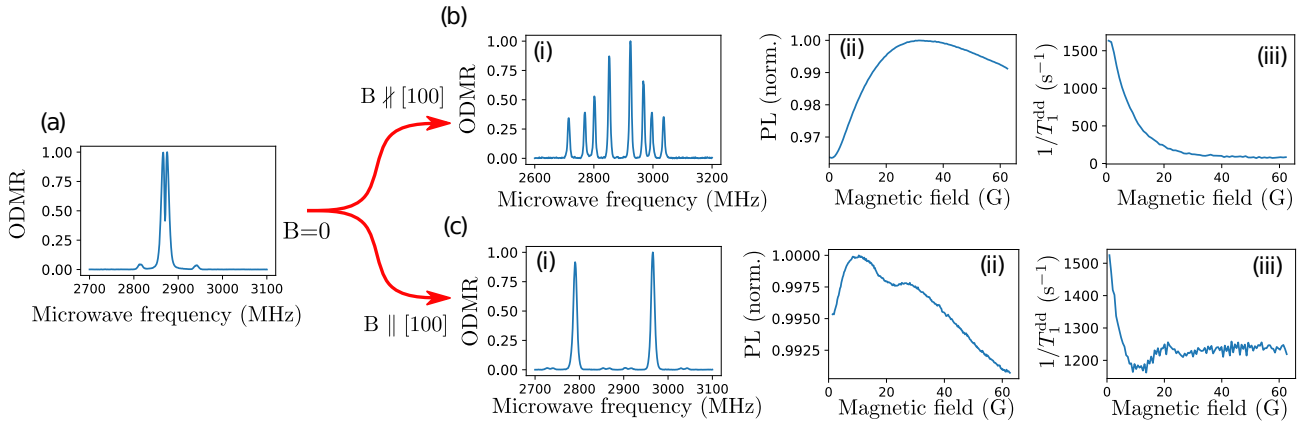

FIG. 3. (a) ODMR spectrum in zero field. (b)-i) ODMR spectrum for a magnetic field ≈ 60 G, misaligned by $\sim 24°$ from the [100] axis. (b)-ii) Normalized photoluminescence of the NV^- ensemble as a function of the magnetic field amplitude. (b)-iii) Stretched part of the spin decay $1/T_1^{dd}$ as a function of the magnetic field amplitude. (c)-i), (c)-ii) and (c)-iii) : same measurements but with a magnetic field close to the [100] axis

terms such as $\langle 0,+1|\mathcal{H}^{dd}|+1,0\rangle$. In zero magnetic field however, we have to take into account these two other mechanisms of the dipolar Hamiltonian in consideration. It was shown in [16] that local electric fields coming from charge traps such as P_1^+ and NV^- centers are responsible for the optically detected spin resonance profile at zero magnetic field in large NV ensembles. Magnetic field noise comes in to second order in zero field. We will then consider the following spin Hamiltonian for the electric field dependent NV^- ground state :

$$\mathcal{H}_{\text{elec}} = d_\perp \left[E_x(S_y^2 - S_x^2) + E_y(S_xS_y + S_yS_x)\right] \qquad (2)$$

where $E_{x,y}$ are the projections of local electric fields on the NV axes. Under local electric fields with orientations given by the angle $\phi_E = \tan(E_x/E_y)$, the eigenstates of H_{NV} are $|0\rangle$ and $|\pm\rangle = \frac{1}{\sqrt{2}}(|+1\rangle \pm e^{-i\phi_E}|-1\rangle)$. Computing the flip-flop terms $|\pm,0\rangle\langle 0,\pm|$ in the fluctuator model shows that $1/T_1^{dd}$ should be increased at zero field, even after averaging over all possible orientations ϕ_E (see SI). Another mechanism at stake when considering dipolar interactions with spin-1 systems are double-flip processes. These processes correspond to terms like $|+1,0\rangle\langle 0,-1|$ in the anisotropic (?) dipolar interaction, giving rise to an exchange of two units of spin-angular momentum. These processes can become significant when the states ± 1 are degenerate and are thus likely to explain part of the zero-field dip in Fig. c)-ii).

In order to discriminate the role of these two effects in the low-field region, we performed another similar study under a purely transverse magnetic field. This regime in fact emulates the effect of the electric field while turning off the resonance condition for double flip processes : indeed for relatively weak transverse magnetic field, the eigen-basis of the spin Hamiltonian is close to $|0\rangle, |+\rangle, |-\rangle$. This property has been used to observe a linear dependence in the electric field for the spin transition frequencies by applying an external transverse magnetic field [5, 22]. Fig. 4 (a) shows the energy levels for the three eigenstates of the NV spin Hamiltonian as a function of a purely transverse magnetic field. We will denote these eigenstates in the general case $|g\rangle$, $|d\rangle$ and $|e\rangle$. For weak transverse magnetic field, $|g\rangle \approx |0\rangle$, $|d\rangle = |-\rangle$ and $|e\rangle \approx |+\rangle$. As the magnetic field increases, $|g\rangle$ and $|e\rangle$ starts to become a mixing of $|0\rangle$ and $|+\rangle$ while $|d\rangle$ remains equal to $|-\rangle$.

Crucially, mixing remains even when the associated energy splitting of the $|d\rangle$ and $|e\rangle$ states is large : Fig. 4-(b) shows both the splitting between the energy levels of $|d\rangle$ and $|e\rangle$, and the matching factor $|\langle e|+\rangle|^2$ characterizing the closeness of the states $\langle e|$ and $\langle +|$. We can see that at a field value of $\sim$ 130 G, the splitting between the $|d\rangle$ and $|e\rangle$ reaches $\sim$ 50 MHz, far exceeding the range of the dipole-dipole resonant coupling (see details in SI), but $|\langle e|+\rangle|^2 > 0.98$ meaning that the spin Hamiltonian eigenstates are still roughly in the $|0\rangle, |+\rangle, |-\rangle$ basis. We can therefore decouple the effects of the double-flip processes $\propto |g,d\rangle\langle d,e|$, which are no longer resonant when $|\boldsymbol{B}| \geq 100$ G, from the effects of the mixing induced by the transverse electric - or in this case magnetic - field.

Fig. 4-(c) shows the measurement of the stretched lifetime T_1^{dd} for a single class of NV centers exposed to a transverse magnetic field between 20 and 130 G on another sample HPHT-150-2, upon which we measured a stretched decay $1/T_1^{dd} = 25 \pm 5$ Hz in the case of strong longitudinal magnetic field. The detuning $\Delta\nu$ between the two states $|d\rangle$ and $|e\rangle$ was measured through ODMR. We attribute the decrease in the spin decay rate when the detuning increases to the loss of effectiveness of the double-flip processes. We can notice that the decay rate reaches a plateau for $\Delta\nu \geq 30$ MHz with a value $1/T_1^{dd} = 57 \pm 5$ Hz about twice as large as the decay rate for a longitudinal magnetic field. This plateau we attribute to the effect of the transverse magnetic field, which we assume to be similar to the effect of the electric field in the low magnetic field regime. We should note that the effect of the double-flip processes is about

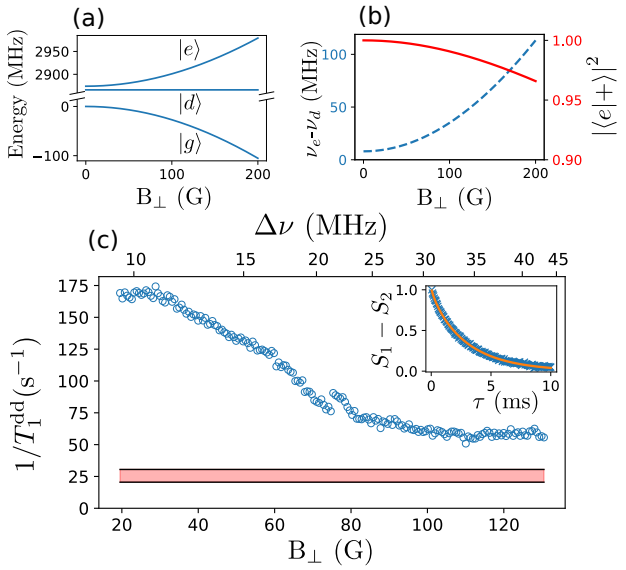

FIG. 4. (a) Energies for the spin Hamiltonian in the presence of pure transverse magnetic field $B_\perp$. The three spin levels are denoted $|g\rangle$, $|d\rangle$ and $|e\rangle$. (b) Blue dashed curve : frequency detuning $\Delta\nu$ between the $|e\rangle$ and $|d\rangle$ states. Red plain curve : Matching factor $|\langle e|+\rangle|^2$ between the states $\langle e|$ and $\langle +|$. (c) Measurement of the stretched exponential decay rate $1/T_1^{\rm dd}$ for a single class as a function of the measured detuning $\Delta\nu$ between the two transitions $|g\rangle \rightarrow |d\rangle$ and $|g\rangle \rightarrow |e\rangle$ for purely transverse magnetic field. The green dashed line correspond to the decay rate for the same class when the magnetic field is longitudinal

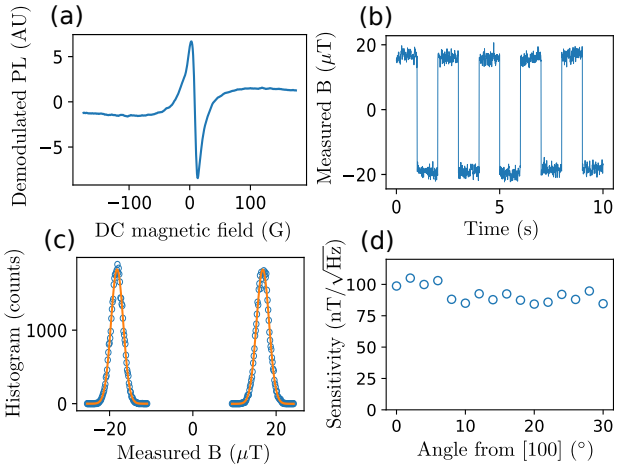

FIG. 5. Low field magnetometry protocol. (a) Demodulated photoluminescence as a function of an externally applied magnetic field with an additional oscillatory magnetic field. (b) Measured magnetic field when alternating a small external magnetic field offset. (c) Histogram of the measurement in Fig. (b) fitted with gaussians of standard deviation $\sigma = 1.5$ μT. (d) Measured sensitivity as function of the angle between the external magnetic field and the [100] crystalline axis.

5 times more important in the depolarization rate than the effect of the electric field, even though the states are not initially fully resonant.

Based on an extension of the fluctuator model developed in SI, we predict an overall increase by a factor of ~ 4 of the dipole-dipole induced decay rate in the non-magnetic basis $|0\rangle, |+\rangle, |-\rangle$ compared to the magnetic basis $|0\rangle, |+1\rangle, |-1\rangle$. While the measured increase is smaller than the predicted one, the measurements agrees with the theoretical increase in the flip-flop rate in the $|+/-\rangle$ basis compared to the $|\pm 1\rangle$ basis.

Similarly, we compute the predicted decay rate when $\boldsymbol{B} \parallel [100]$ case compared when $\boldsymbol{B} = 0$, and find a theoretical increase of $\sim 20\%$ when $\boldsymbol{B} = 0$ due to the mixing by the local electric field. This, along with the double-flip processes explains the behavior observed in Fig. 3 (c)-ii) and (c)-iii).

Our observations have important implications for magnetometry with NV ensembles. DC microwave-free magnetometry has already been performed using either NV-NV cross-relaxations [1, 2] or level anti-crossing [25–27]. Here we propose to perform a similar protocol , but using the spin depolarization at zero-field as proposed in [8, 9]. The main advantage with the previously mentioned protocols is the fact that the sensitivity does not depend crucially on crystalline orientation, making this protocol applicable with diamond powders or polycrystalline samples.

Fig. 5 (a) shows the demodulated PL as a DC magnetic field is scanned in a random direction and an additional alternating magnetic field of amplitude ~ 10 G and frequency ~ 1 kHz is added through the same electromagnet. The sample used here is HPHT-15-1 and the laser power ~ 1 mW. We can see a sharp linear slope in low field $|B| < 5$ G. Once calibrated, in this case with ODMR, the slope can provide a 1D magnetic field measurement, which could be extended to 3D with a set of 3 coils or 3 electromagnets, as in [27]. In order to assess the sensitivity of the measurement, we alternate a small DC field of ≈ 40 μT every few seconds and take a histogram of the measured fields, as shown in Fig. 5 (b) and (c). The histogram is well fitted with gaussians of standard deviation $\sigma = 1.5$ μT. The measurement was performed here with an output low-pass filter of time constant $\tau = 3$ ms, which gives us a sensitivity $\eta = \sigma\sqrt{\tau} = 82$ nT/$\sqrt{\rm Hz}$.

We now evaluate the relative role of the three causes of spin depolarization in the magnetometer, namely the splitting of the classes, the local electric field and the double-flip processes. In order to do so, we measure the magnetometer sensitivity while changing the angle of the magnetic field. The results are shown in Fig. 5 (d). We can see a slight increase of $\sim 10\%$ in the sensitivity as we leave the [100] region, but overall the sensitivity remains relatively flat. When $\boldsymbol{B}$ is aligned with the [100] crystalline axis, only the double flips and the electric field cause a depolarization, whereas in every other orientation the three effects are at play. The double-flips and electric field effects are thus the dominant factors in the

sensitivity of this protocol. While it may seem surprising that the effects with a lower contribution on the PL contrast have a higher effect on this PL-based protocol, what matters here is not the absolute contrast but the slope of the change of contrast with respect to the magnetic field. The latter is in fact larger for the local electric field and double flips processes than for the process involving only flip-flops. It should be noted that this observation is sample dependent, and that other samples, including from the same batch, have shown a higher orientation dependence, corresponding to a lower contribution from the electric field and double-flip processes.

As a conclusion, we identified three mechanisms causing extra spin depolarization in zero field for dense ensemble of NV^- centers, all related to an increase in the dipole-dipole induced cross-relaxations between the spins of NV centers. The lift in degeneracy of the spin state of different NV classes was found to be the main cause of zero-field depolarization, followed by double-flip processes and then the electric field induced mixing. We have employed cross-relaxation for microwave and orientation-free DC-magnetometry and demonstrated a sensitivity below 100 $\mathrm{nm}/\sqrt{\mathrm{Hz}}$ for a single 10 μm commercially available diamond and show that that double-flips and electric field play an important role. Besides magnetometry, our work offers prospects for understanding many body phenomena with strongly coupled spins.

ACKNOWLEDGEMENTS

[1] Rinat Akhmedzhanov, Lev Gushchin, Nikolay Nizov, Vladimir Nizov, Dmitry Sobgayda, Ilya Zelensky, and Philip Hemmer. Microwave-free magnetometry based on cross-relaxation resonances in diamond nitrogen-vacancy centers. *Phys. Rev. A*, 96(1):013806, July 2017. Number: 1.

[2] Rinat Akhmedzhanov, Lev Gushchin, Nikolay Nizov, Vladimir Nizov, Dmitry Sobgayda, Ilya Zelensky, and Philip Hemmer. Magnetometry by cross-relaxation-resonance detection in ensembles of nitrogen-vacancy centers. *Phys. Rev. A*, 100(4):043844, October 2019. Number: 4.

[3] Georgios Chatzidrosos, Joseph Shaji Rebeirro, Huijie Zheng, Muhib Omar, Andreas Brenneis, Felix M Stürner, Tino Fuchs, Thomas Buck, Robert Rölver, Tim Schneemann, et al. Fiberized diamond-based vector magnetometers. *Frontiers in Photonics*, page 4, 2021.

[4] Joonhee Choi, Soonwon Choi, Georg Kucsko, Peter C Maurer, Brendan J Shields, Hitoshi Sumiya, Shinobu Onoda, Junichi Isoya, Eugene Demler, Fedor Jelezko, et al. Depolarization dynamics in a strongly interacting solid-state spin ensemble. *Physical review letters*, 118(9):093601, 2017.

[5] Florian Dolde, Helmut Fedder, Marcus W Doherty, Tobias Nöbauer, Florian Rempp, Gopalakrishnan Balasubramanian, Thomas Wolf, Friedemann Reinhard, Lloyd CL Hollenberg, Fedor Jelezko, et al. Electric-field sensing using single diamond spins. *Nature Physics*, 7(6):459–463, 2011.

[6] Andrew M Edmonds, Connor A Hart, Matthew J Turner, Pierre-Olivier Colard, Jennifer M Schloss, Kevin S Olsson, Raisa Trubko, Matthew L Markham, Adam Rathmill, Ben Horne-Smith, et al. Characterisation of cvd diamond with high concentrations of nitrogen for magnetic-field sensing applications. *Materials for Quantum Technology*, 1(2):025001, 2021.

[7] RJ Epstein, FM Mendoza, YK Kato, and DD Awschalom. Anisotropic interactions of a single spin and dark-spin spectroscopy in diamond. *Nature physics*, 1(2):94–98, 2005.

[8] DS Filimonenko, VM Yasinskii, Alexander P Nizovtsev, S Ya Kilin, and Fedor Jelezko. Manifestation in irluminescence of cross relaxation processes between nv-centers in weak magnetic fields. *Journal of Applied Spectroscopy*, 88(6):1131–1143, 2022.

[9] DS Filimonenko, VM Yasinskii, AP Nizovtsev, and S Ya Kilin. Weak magnetic field resonance effects in diamond with nitrogen-vacancy centers. *Semiconductors*, 52(14):1865–1867, 2018.

[10] R. Giri, C. Dorigoni, S. Tambalo, F. Gorrini, and A. Bifone. Selective measurement of charge dynamics in an ensemble of nitrogen-vacancy centers in nanodiamond and bulk diamond. *Phys. Rev. B*, 99(15):155426, April 2019. Number: 15.

[11] R. Giri, F. Gorrini, C. Dorigoni, C. E. Avalos, M. Cazzanelli, S. Tambalo, and A. Bifone. Coupled charge and spin dynamics in high-density ensembles of nitrogen-vacancy centers in diamond. *Phys. Rev. B*, 98(4):045401, July 2018. Number: 4.

[12] A. Jarmola, V. M. Acosta, K. Jensen, S. Chemerisov, and D. Budker. Temperature- and Magnetic-Field-Dependent Longitudinal Spin Relaxation in Nitrogen-Vacancy Ensembles in Diamond. *Phys. Rev. Lett.*, 108(19):197601, May 2012. Number: 19.

[13] A. Jarmola, A. Berzins, J. Smits, K. Smits, J. Prikulis, F. Gahbauer, R. Ferber, D. Erts, M. Auzinsh, and D. Budker. Longitudinal spin-relaxation in nitrogen-vacancy centers in electron irradiated diamond. *Appl. Phys. Lett.*, 107(24):242403, December 2015. Number: 24.

[14] Georg Kucsko, Soonwon Choi, Joonhee Choi, Peter C Maurer, Hengyun Zhou, Renate Landig, Hitoshi Sumiya, Shinobu Onoda, Junich Isoya, Fedor Jelezko, et al. Critical thermalization of a disordered dipolar spin system in diamond. *Physical review letters*, 121(2):023601, 2018.

[15] Ngoc Diep Lai, Dingwei Zheng, Fedor Jelezko, François Treussart, and Jean-François Roch. Influence of a static magnetic field on the photoluminescence of an ensemble of nitrogen-vacancy color centers in a diamond single-crystal. *Applied Physics Letters*, 95(13):133101, 2009.

[16] Thomas Mittiga, Satcher Hsieh, Chong Zu, Bryce Kobrin, Francisco Machado, Prabudhya Bhattacharyya, NZ Rui, Andrey Jarmola, Soonwon Choi, Dmitry Budker, et al. Imaging the local charge environment of

nitrogen-vacancy centers in diamond. *Physical review letters*, 121(24):246402, 2018.

[17] Mariusz Mrózek, Adam M Wojciechowski, and Wojciech Gawlik. Characterization of strong nv- gradient in the e-beam irradiated diamond sample. *Diamond and Related Materials*, 120:108689, 2021.

[18] Mariusz Mrózek, Daniel Rudnicki, Pauli Kehayias, Andrey Jarmola, Dmitry Budker, and Wojciech Gawlik. Longitudinal spin relaxation in nitrogen-vacancy ensembles in diamond. *EPJ Quantum Technol.*, 2(1):22, December 2015. Number: 1.

[19] A Norambuena, E Muñoz, HT Dinani, A Jarmola, Patrick Maletinsky, Dmitry Budker, and JR Maze. Spin-lattice relaxation of individual solid-state spins. *Physical Review B*, 97(9):094304, 2018.

[20] C Pellet-Mary, P Huillery, M Perdriat, and G Hétet. Magnetic torque enhanced by tunable dipolar interactions. *Physical Review B*, 104(10):L100411, 2021.

[21] Clément Pellet-Mary, Paul Huillery, Maxime Perdriat, A Tallaire, and Gabriel Hétet. Optical detection of paramagnetic defects in diamond grown by chemical vapor deposition. *Physical Review B*, 103(10):L100411, 2021.

[22] Ziwei Qiu, Assaf Hamo, Uri Vool, Tony X Zhou, and Amir Yacoby. Nanoscale electric field imaging with an ambient scanning quantum sensor microscope. *arXiv preprint arXiv:2205.03952*, 2022.

[23] DA Redman, S Brown, RH Sands, and SC Rand. Spin dynamics and electronic states of n-v centers in diamond by epr and four-wave-mixing spectroscopy. *Physical review letters*, 67(24):3420, 1991.

[24] Alexandre Tallaire, Ovidiu Brinza, Paul Huillery, Tom Delord, Clément Pellet-Mary, Robert Staacke, Bernd Abel, Sébastien Pezzagna, Jan Meijer, Nadia Touati, Laurent Binet, Alban Ferrier, Philippe Goldner, Gabriel Hetet, and Jocelyn Achard. High nv density in a pink cvd diamond grown with n2o addition. *Carbon*, 170:421 – 429, 2020.

[25] Arne Wickenbrock, Huijie Zheng, Lykourgos Bougas, Nathan Leefer, Samer Afach, Andrey Jarmola, Victor M. Acosta, and Dmitry Budker. Microwave-free magnetometry with nitrogen-vacancy centers in diamond. *Applied Physics Letters*, 109(5):053505, 2016.

[26] Huijie Zheng, Georgios Chatzidrosos, Arne Wickenbrock, Lykourgos Bougas, Reinis Lazda, Andris Berzins, Florian Helmuth Gahbauer, Marcis Auzinsh, Ruvin Ferber, and Dmitry Budker. Level anti-crossing magnetometry with color centers in diamond. In *Slow Light, Fast Light, and Opto-Atomic Precision Metrology X*, volume 10119, pages 115–122. SPIE, 2017.

[27] Huijie Zheng, Zhiyin Sun, Georgios Chatzidrosos, Chen Zhang, Kazuo Nakamura, Hitoshi Sumiya, Takeshi Ohshima, Junichi Isoya, Jörg Wrachtrup, Arne Wickenbrock, and Dmitry Budker. Microwave-Free Vector Magnetometry with Nitrogen-Vacancy Centers along a Single Axis in Diamond. *Phys. Rev. Applied*, 13(4):044023, April 2020. Number: 4.

[28] Hengyun Zhou, Joonhee Choi, Soonwon Choi, Renate Landig, Alexander M Douglas, Junichi Isoya, Fedor Jelezko, Shinobu Onoda, Hitoshi Sumiya, Paola Cappellaro, et al. Quantum metrology with strongly interacting spin systems. *Physical review X*, 10(3):031003, 2020.